HYBRID RENEWABLE WITH CONTROL STRATEGIES IN STANDALONE DC AND AC MICROGRIDS FOR ENERGY MANAGEMENT

[1]M.MURALI KRISHNA, [2]D.MAHESWARA REDDY

[1]Associate Professor & HOD, [2] PG student

[1]Dept of EEE, [1]BHEEMA INSTITUTE OF TECHNOLOGY & SCIENCE, ADONI RD, DHANAPURAM, AP,INDIA

_____

Abstract: Energy management strategies are becoming essential for the power sharing and voltage regulation purposes. The classical energy management strategies employ the maximum power point tracking (MPPT) algorithms and rely on batteries in case of possible excess or deficit of energy. However, in order to realize constant current-constant voltage (IU) charging regime and increase the life span of batteries, energy management strategies require being more flexible with the power curtailment feature. In this paper, a coordinated and multivariable energy management strategy is proposed that employs a wind turbine and a photovoltaic array of a standalone DC microgrid as controllable generators by adjusting the pitch angle and the switching duty cycles. The proposed strategy is developed as an online nonlinear model predictive control algorithm. Applying to a sample standalone dc microgrid, the developed controller realizes the IU regime for charging the battery bank. The variable load demands are also shared accurately between generators in proportion to their ratings. Moreover, the DC bus voltage is regulated within a predefined range, as a design parameter. The control technique is simulated using MATLAB/SIMULINK in PV- wind power generating system with MPPT and case study has been done on the control strategy and verifies the effectiveness of adaptive droop control on output converter voltage.

_____

I. INTRODUCTION

The near future distribution networks will consist of several interconnected microgrids that will locally generate, consume, and store energy [1]. A microgrid may operate as an extension of the main grid, i.e., grid-connected, or as a standalone network with no connection to the grid. Standalone dc microgrids have some distinct applications in avionic, automotive, or marine industries, as well as remote rural areas. While ac systems suffer from the need of synchronization of several generators [2], [3], dc microgrids are more efficient due to the fact that dc generators and storages do not need ac-dc converters for being connected to dc microgrids [4], [1]. The three well-known issues regarding voltage regulation, power sharing, and battery management, are more severe in standalone green microgrids, that consist of only intermittent solar and wind energy sources, and lead to the necessity of more sophisticated control strategies. The stability of a dc microgrid is measured in terms of the stability of its dc bus voltage level [5], [6], which is one of the main control objectives. The grid voltage source converters (G-VSCs) are the primary slack terminals to regulate the voltage level of grid-connected microgrids (e.g., [5], [6]). Battery banks, on the other hand, are effective slack terminals for standalone microgrids [6]; however, their energy absorbing capacities are limited regarding a number of operational constraints, as explained later in this section. In order to regulate the voltage level of standalone dc microgrids, the works in [2] and [6] present load-shedding strategies for the cases in which there is insufficient power generation or energy storage. The works in [1], on the other hand, present strategies that curtail the renewable power generations of standalone dc microgrids if the battery bank cannot absorb the excess generation. These curtailment strategies restrict the batteries charging rate by the maximum absorbing power; however, the maximum charging current must also be limited. Furthermore, they do not curtail the power of each generator in proportion to its rating. In order to prevent over-stressing conditions and circulating currents between generators [13], load demands need to be shared between all slack DGs in proportion to their ratings [7]. The works in [3] extend the conventional droop control technique [1] for dc slack terminals by replacing the conventional curves with either a dc power-dc voltage or a dc voltage-output current curve. However, standalone dc microgrids are usually located in small-scale areas where the power sharing between DGs can be managed by centralized algorithms, which are less affected by two issues:

1) batteries in charging mode are nonlinear loads causing distortions to the grid voltage; and
 2) the absolute voltage level of a standalone microgrid is shifted as the result of the load demand variation. A number of phenomena affect the batteries operation during the charging mode [9]:

_____

1) applying high charging currents, the batteries voltages quickly reach to the gassing threshold;

2) the internal resistor and hence power losses and thermal effects increase at high SOC levels; and

3) batteries cannot be fully charged with a constant high charging current. The work in [6] limits, as an operational constraint, the maximum absorbed power by the batteries in order to protect them from being overcharged. However, since batteries act as nonlinear loads during the charging mode, it does not necessarily limit the charging currents. Alternatively, the works in [1] restricts the maximum attainable SOC that leads to unused capacities. Depending on the proportion of the power generation to the load demand ratio within standalone DC microgrids, three cases are envisaged:

1) power generation and load demand are balanced; 2) load demand exceeds power generation causes dc bus voltage to drop in absence of any load shedding; and 3) power generation is higher than load demand leads batteries to be overcharged and bus voltage to climb. This study focuses on case 3) in which the generated power must be curtailed if it violates the batteries charging rates or if batteries are fully charged. A novel energy management strategy (EMS) is proposed to address, as its control objectives, three aforementioned issues corresponding standalone dc microgrids; i.e., dc bus voltage regulation, proportional power sharing, and battery management. In contrast to the strategies available in literature in which renewable energy systems (RESs) always operate in their MPPT mode, the proposed multivariable strategy uses a wind turbine and a PV array as controllable generators and curtails their generations if it is necessary. The proposed EMS is developed as an online novel NMPC strategy that continuously solves an optimal control problem (OCP) and finds the optimum values of the pitch angle and three switching duty cycles. It simultaneously controls four variables of microgrids: 1) power coefficient of the wind turbine; 2) angular velocity of the wind generator; 3) operating voltage of the PV array; and 4) charging current of the battery bank. It is shown that, employing new available nonlinear optimization techniques and tools, the computational time to solve the resulting NMPC strategy is in permissible range. Unlike dump load-based strategies that only protect the battery from overcharging, the proposed strategy implements the IU charging regime that helps to increase the batteries life span. Moreover, removing dump loads, the overall installation cost is reduced.

II.DISTRIBUTED GENERATION

Distributed energy, also district or decentralized energy is generated or stored by a variety of small, grid-connected devices referred to as distributed energy resources (DER) or distributed energy resource systems. Conventional power stations, such as coal-fired, gas and nuclear powered plants, as well as hydroelectric dams and large-scale solar power stations, are centralized and often require electricity to be transmitted over long distances. By contrast, DER systems are decentralized, modular and more flexible technologies, that are located close to the load they serve, albeit having capacities of only 10 megawatts (MW) or less.

Fig 1 Local wind generator, Spain, 2010

DER systems typically use renewable energy sources, including small hydro, biomass, biogas, solar power, wind power, and geothermal power, and increasingly play an important role for the electric power distribution system. A grid-connected device for electricity storage can also be classified as a DER system, and is often called a distributed energy storage system (DESS). By means of an interface, DER systems can be managed and coordinated within a smart grid. Distributed generation and storage enables collection of energy from many sources and may lower environmental impacts and improve security of supply.

III.ENERGY STORAGE SYSTEM

A distributed energy resource is not limited to the generation of electricity but may also include a device to store distributed energy (DE). Distributed energy storage systems (DESS) applications include several types of battery, pumped hydro, compressed air, and thermal energy storage.

3.1 Flywheels

An advanced flywheel energy storage (FES) stores the electricity generated from distributed resources in the form of angular kinetic energy by accelerating a rotor (flywheel) to a very high speed of about 20,000 to over 50,000 rpm in a vacuum enclosure. Flywheels can respond quickly as they store and feed back electricity into the grid in a matter of minutes.

3.2 Vehicle-to-grid

Future generations of electric vehicles may have the ability to deliver power from the battery in a vehicle-to-grid into the grid when needed. An electric vehicle network has the potential to serve as a DESS.

3.3 PV storage

Common battery technologies used in today's PV systems include, the valve regulated lead-acid battery (lead–acid battery), nickel–cadmium and lithium-ion batteries. Compared to the other types, lead-acid batteries have a shorter lifetime and lower energy density. However, due to their high reliability, low self-discharge (4-6% per year) as well as low investment and maintenance costs, they are currently the predominant technology used in small-scale, residential PV systems, as lithium-ion batteries are still being developed and about 3.5 times as expensive as lead-acid batteries. Furthermore, as storage devices for PV systems are used stationary, the lower energy and power density and therefore higher weight of lead-acid batteries are not as critical as for electric vehicles. However, lithium-ion batteries, such as the Tesla Power wall, have the potential to replace lead-acid batteries in the near future, as they are being intensively developed and lower prices are expected due to economies of scale provided by large production facilities such as the Giga factory 1. In addition, the Li-ion batteries of plug-in electric cars may serve as a future storage devices, since most vehicles are parked an average of 95 percent of the time, their batteries could be used to let electricity flow from the car to the power lines and back. Other rechargeable batteries that are considered for distributed PV systems include, sodium–sulfur and vanadium redox batteries, two prominent types of a molten salt and a flow battery, respectively.

IV.OUTLINE OF DC MICROGRID

A schematic of the dc microgrid with the conventions employed for power is given in Fig. 2. The dc bus connects wind energy conversion system (WECS), PV panels, multilevel energy storage comprising battery energy storage system (BESS) and super capacitor, EV smart charging points, EV fast charging station, and grid interface. The WECS is connected to the dc bus via an ac–dc converter. PV panels are connected to the dc bus via a dc–dc converter. The BESS can be realized through flow battery technology connected to the dc bus via a dc–dc converter. The super capacitor has much less energy capacity than the BESS. Rather, it is aimed at compensating for fast fluctuations of power and so provides cache control as detailed in [6].
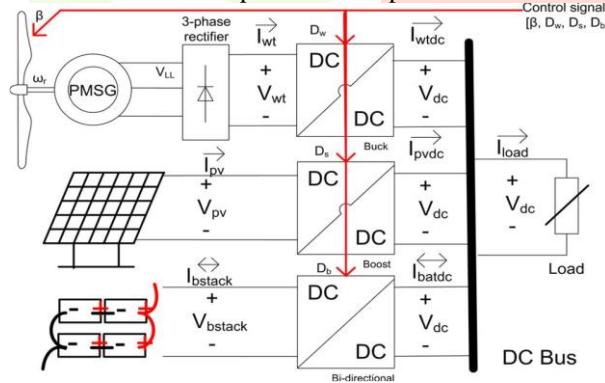

Fig.2. Layout of the dc microgrid

Fig. 3 Wind and PV-based power generation for the vertically integrated microgrid

4.1 OVER VIEW

Thanks to the multilevel energy storage, the intermittent and volatile renewable power outputs can be managed, and a deterministic controlled power to the main grid is obtained by optimization. Providing uninterruptible power supply (UPS) service to loads when needed is a core duty of the urban microgrid. EV fast charging introduces a stochastic load to the microgrid. The multilevel energy storage mitigates potential impacts on the main grid. In building integration, a vertical axis wind turbine may be installed on the rooftop as shown in Fig. 3. PV panels can be co-located on the rooftop and the facade of the building. Such or similar configurations benefit from a local availability of abundant wind and solar energy. The fast charging station is realized for public access at the ground level. It is connected close to the LV–MV transformer to reduce losses and voltage drop. EVs parked in the building are offered smart charging within user-defined constraints.

4.2 Operational Optimization of Microgrid Renewable Energy Integration

The algorithm for optimized scheduling of the microgrid is depicted in Fig. 4. In the first stage, wind and solar power generation are forecast. The uncertainty of the wind and solar power is presented by a three-state model. An example of such a forecast is shown in Fig. 4. State 1 represents a power forecast lower than the average power forecast. This state is shown by the power forecast of _P1 with the forecast probability of _pr1 assigned to it. The average power forecast and the probability of forecast assigned to it give state 2.
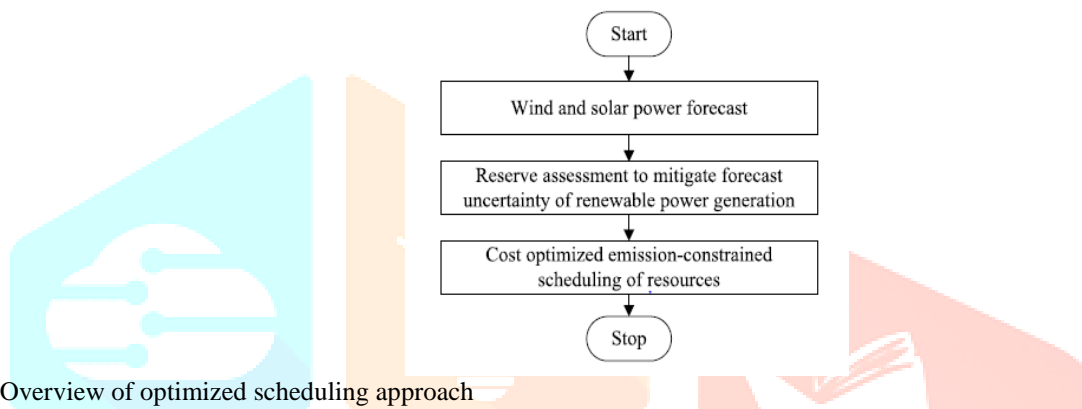
Fig. 4 Overview of optimized scheduling approach

State 3 represents a power forecast higher than the average power forecast. Then, wind and solar power forecasts are aggregated to produce the total renewable power forecast model. This aggregation method is formulated in Section III-A. The aggregated power generation data are used to assign hourly positive and negative energy reserves to the BESS for the microgrid operation. The positive energy reserve of the BESS gives the energy stored that can be readily injected into the dc bus on demand. The negative energy reserve gives the part of the BESS to remain uncharged to capture excess power on demand. Energy reserve assessment is performed according to the aggregated renewable power generation forecast. In order to compensate for the uncertainty of the forecast, a method is devised to assess positive and negative energy reserves . Finally, the emission constrained cost optimization is formulated to schedule the microgrid resources for the day-ahead dispatch. The optimized scheduling is formulated in Section III-C.

TABLE I EXAMPLE A: WIND AND SOLAR POWER FORECAST DATA

Individual state	State 1	State 2	State 3
Wind forecast probability	0.25	0.50	0.25
Wind power (kW)	40	50	60
Solar forecast probability	0.25	0.50	0.25
Solar power (kW)	15	20	25

4.3 Energy Reserve Assessment for Operation of Microgrid

Taking into account the aggregated wind and solar power forecast model developed above, an illustrative example is provided to show how the energy reserve is assessed. In Table IV, an aggregated three-state power forecast model for three continuous hours is assumed. The aggregated power forecast for hour 1 is taken from the example solved. The aggregated power forecast of hours 2 and 3 is calculated by the same method. As shown in Table I, the probability of having real-time power output at state 1 in three continuous hours is equal to the product of the probabilities in state 1 for those three hours.

4.4 Formulation of Optimized Scheduling of Microgrid

The objective of the optimization is to minimize operation cost of the microgrid in interconnected mode and provide UPS service in the autonomous mode. These objectives can be achieved by minimization of the following defined objective function:

$$F(P_G, P_{EVS}) = \sum_{i=1\,h}^{T} C_{1kWh}(i) \times P_G(i) \times \tau_h$$
$$+ \sum_{i=1\,h}^{T} C_{1kWh}(i) \times P_{EVS}(i) \times \tau_h$$
$$+ \sum_{i=1\,h}^{T} EPBF \times \overline{EMS} \times P_G(i) \times \tau_h$$

where F is the objective function to be minimized, T is the scheduling horizon of the optimization, τh is the optimization time step which is 1 h, C1kWh is the energy cost for 1 kWh energy, PG is the incoming power from the grid, PEVS is the smart charging power for EVs, EPBF is the emission penalty– bonus factor for CO2, and EMS is the average CO2 emission of 1 kWh electrical energy in the power system outside the microgrid. In this objective function, PG and PEVS are to be determined by optimization. The first term in the objective function above expresses the energy cost, the second term defines the cost of EV smart charging, and the third term describes the emission cost. As shown in Fig. 1, for positive values of PG, the microgrid draws power from the main grid, and for negative values of PG the microgrid injects power into the main grid. The emission term penalizes power flow from the main grid to the microgrid. If the microgrid draws power from the main grid, the microgrid would contribute to emissions of the power system. On the other hand, as the microgrid has no unit that produces emission, when the microgrid returns power to the main grid, it contributes to emission reduction. The optimization program determines a solution that minimizes the operation cost of the dc microgrid.

4.5 ADAPTIVE DROOP CONTROL OF BESS

In this section, the real-time operation of the microgrid in the interconnected and autonomous modes is studied. In the interconnected mode of operation, an adaptive droop control is devised for the BESS. The adaptive droop characteristic of the BESS power electronic converter is selected on the basis of the deviation between the optimized and real-time SOC of the BESS, as calculated in Section III. Details of the method are provided in Section IV-A. In autonomous mode of operation, the BESS is responsible for keeping the voltage of the dc bus
in a defined acceptable range for providing UPS service.

$$f_1 = V_{dc}\left(I_{pvdc} + I_{wtdc} + I_{batdc} - I_{load}\right), \qquad (2a)$$
$$f_2 = V_{dc} - I_{load}R_L. \qquad (2b)$$

A. Wind Branch

Performance of the wind turbines is measured as the power coefficient curve with respect to the tip speed ratio and pitch angle [3]. Equation (3) shows the power coefficient curve of three-blade wind turbines [4]:

$$f_3 = C_{p,norm} - \frac{1}{C_{p,max}} \times$$
$$(C_1(\frac{C_2}{\lambda_i} - C_3\beta - C_4)\exp(-\frac{C_5}{\lambda_i}) + C_6\lambda),$$
$$f_4 = \lambda - \frac{Rad \times \omega_r}{U_x},$$
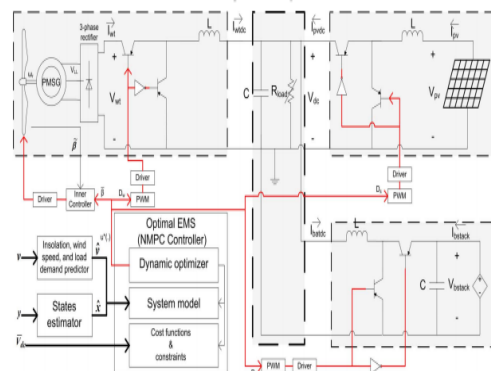$$f_5 = \lambda_i - (\frac{1}{\lambda + 0.08\beta} - \frac{0.035}{\beta^3 + 1})^{-1},$$

Fig. 5 Simplified view of the dc microgrid and the developed NMPC controller. The battery bank is assumed to work in charging mode.

Model predictive control (MPC) is an advanced method of process control that has been in use in the process industries in chemical plants and oil refineries since the 1980s. In recent years it has also been used in power system balancing models.[1] Model predictive controllers rely on dynamic models of the process, most often linear empirical models obtained

by system identification. The main advantage of MPC is the fact that it allows the current timeslot to be optimized, while keeping future timeslots in account. This is achieved by optimizing a finite time-horizon, but only implementing the current timeslot. MPC has the ability to anticipate future events and can take control actions accordingly.PID and LQR controllers do not have this predictive ability. MPC is nearly universally implemented as a digital control, although there is research into achieving faster response times with specially designed analog circuitry.

TABLE II
Wind Turbine, PMSG, Battery Stack, and PV Parameters in This Study

Wind turbine		PMSG		Battery stack		PV array	
$C_1(-)$	0.517	$J(Kg.m^2)$	0.35	$C_{max}(Ah)$	48.15	$R_s(\Omega)$	0.221
$C_2(-)$	116.0	$F(N.m.s)$	0.002	$R_{bat}(\Omega)$	0.019	$R_{sh}(\Omega)$	405.4
$C_3(-)$	0.4	$P(-)$	8	$V_0(V)$	12.3024	$n_d(-)$	1.3
$C_4(-)$	5.0	$\psi(V.s)$	0.8	$P_1(-)$	0.9	$N_s(-)$	54
$C_5(-)$	21.0	$P_{rated}(KW)$	10.0	$N_{bats}(-)$	8	$I_{sc,stc}(A)$	8.21
$C_6(-)$	0.007	$L_s(H)$	0.0083	$N_{batp}(-)$	3	$V_{oc,stc}(V)$	32.9
$\lambda_{opt}(-)$	8.1			$T_s(sec)$	0.726	$k_I(A/K)$	0.003
$P_{wt,nom}(KW)$	10.0			$V_{bstack,nom}(V)$	96.0	$k_V(V/K)$	-0.12
Rad (m)	4.01			$P_{bat,nom}(KW)$	1.296	$N_{pvs}(-)$	1
$U_{x,base}(m/s)$	12.0			$C_{10}(Ah)$	45.0	$N_{pvp}(-)$	10
$C_{p,max}(-)$	0.48			$V_{gas}(V)$	13.0	$P_{pv,nom}(KW)$	2.001

V. SIMULATION RESULTS

Table shows the parameters of different components and their values in this study. The linear load demand is also less than or equal to 12 KW. Two test scenarios are carried out to evaluate the performance of the developed optimal EMS. Table III summarizes these test scenarios.

Scenario I: Constant Current Charging Mode:

Fig. illustrates the normalized wind speed, insolation, and load demand inputs to the system. Wind speed starts at the rating value of the generator and sharply increases by 37.5% at s. Load demand is below the nominal value, except between 300 to 600 s. Moreover, solar irradiance is constant during the simulation only for results clarification. Fig.5-8 depicts the calculated optimal control variables. Applying these optimal control variables to standalone dc microgrid, different variables of the wind and solar branches are depicted in Fig. 5. Fig. 6 illustrates the resulting dc bus voltage and the battery bank SOC and charging currents. The wind branch operates at MPPT mode up to seconds with a calculated pitch angle of zero as given in Fig. 8. Fig. 9 shows the calculated buck converter duty cycle that adjusts the rotational speed of the wind turbine at its nominal value, as given by Fig. 10. Fig.11 indicates that the resulting power coefficient reaches to its maximum value. At and 600 s, the pitch angle goes up to 1.2 and 16 degrees, respectively, to promote pitching to feather. Fig. 10 and 11 illustrates a combination of the speed and power coefficient variations that curtails the generation down to KW after s, as given by Fig. 12. Fig. 13 and 14 illustrates that though the PV array initially operates at its MPP, i.e., and , the controller curtails its generation down to KW [Fig. 13] after s. Therefore, the power sharing deficiency in (1) is 0.035% which is within the permissible range of . It should be noted that causes a slight inaccuracy in the wind power generation which can be reduced by decreasing the design parameter . In spite of significant wind speed and load demand variations, Fig. 6 depicts that the dc bus voltage level stays within the permissible range, i.e., . From Fig. 7, it can be seen that after s, when there is not enough generated power to charge battery, controller reduces the dc bus voltage
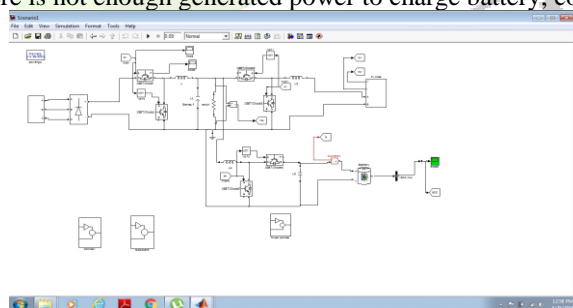

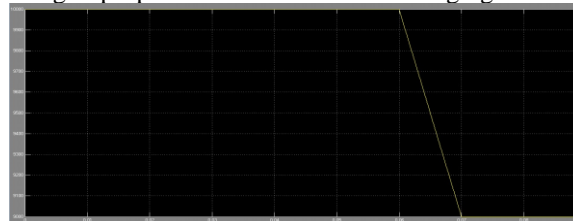Fig 6: proposed Constant Current Charging Mode
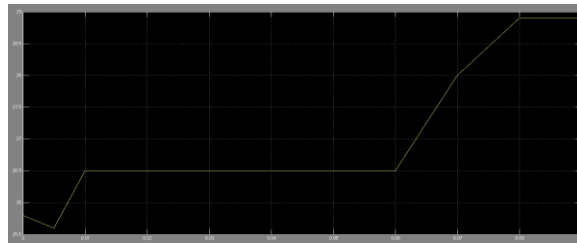

Fig7: wind turbine power
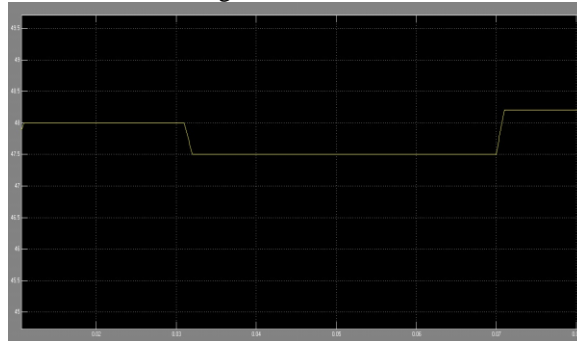
Fig8: Solor current

Fig9: Solor power

Fig10: Dp
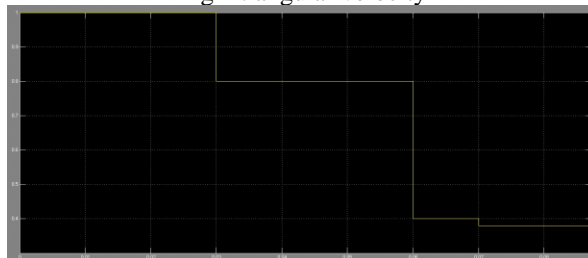

Fig11: angular velocity

Fig12: Cp

A. Scenario II: Constant Voltage Charging Mode

Once the battery terminal voltage reaches the gassing voltage, the charging current should be gradually reduced in order to maintain the voltage below the gassing level and fully charge the battery without the risk of permanent damage. For this purpose,
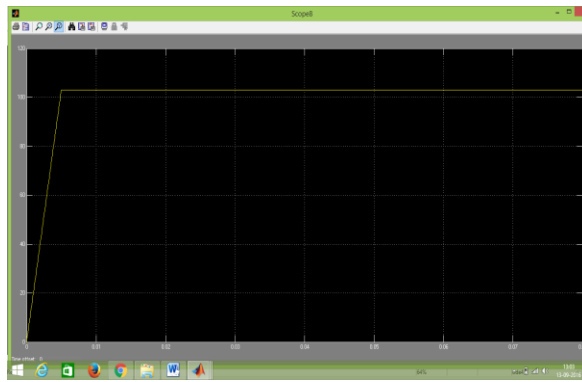
Fig13: Angular velocity

Fig14: SOC

VI.CONCLUSION

An optimal EMS that manages the energy flows across a standalone green dc microgrid, consisting of the wind, solar, and battery branches has proposed. A coordinated and multivariable strategy has been developed to address, as the optimal EMS, three main control objectives of standalone dc microgrids. These objectives are the voltage level regulation, proportional power sharing, and battery management. In order to address these objectives, the developed EMS simultaneously controls the pitch angle of the wind turbine and the switching duty cycles of three dc -dc converters. It has been shown that the developed controller tracks the MPPs of the wind and solar bran ches within the normal conditions and curtails their generations during the under load conditions. The provided flexible generation curtailment strategy realizes the constant current-constant voltage charging regime that potentially increases the life span of the battery bank. It is important to note that the proposed strategy can be employed as a centralized implementation of the primary and secondary levels in the hierarchical architecture. The simulation results have shown its ability to achieve all control objectives. The issue of considering the discharging mode of the battery operation, which shifts the problem to the class of hybrid dynamical systems, is currently being investigated.

REFERENCES

[1] J. M. Guerrero, M. Chandorkar, T. Lee, and P. C. Loh, "Advanced Control Architectures for Intelligent Microgrids-Part I: Decentralized and Hierarchical Control," IEEE Trans. Ind. Electron., vol. 60, no. 4, pp. 1254–1262, 2013.
[2] R. S. Balog, W. W. Weaver, and P. T. Krein, "The load as an energy asset in a distributed DC smartgrid architecture," IEEE Trans. Smart Grid, vol. 3, no. 1, pp. 253–260, 2012.
[3] J. M. Guerrero, P. C. Loh, T. L. Lee, and M. Chandorkar, "Advanced Control Architectures for Intelligent Microgrids-Part II: Power quality, energy storage, and AC/DC microgrids," IEEE Trans. Ind. Electron., vol. 60, no. 4, pp. 1263–1270, 2013.
[4] N. Eghtedarpour and E. Farjah, "Control strategy for distributed integration of photovoltaic and energy storage systems in DC micro-grids," Renew. Energy, vol. 45, no. 0, pp. 96–110, 2012.
[5] D. Chen and L. Xu, "Autonomous DC voltage control of a DC microgrid with multiple slack terminals," IEEE Trans. Power Syst., vol. 27, no. 4, pp. 1897–1905, Nov. 2012.
[6] L. Xu and D. Chen, "Control and operation of a DC microgrid with variable generation and energy storage," IEEE Trans. Power Del., vol. 26, no. 4, pp. 2513–2522, Oct. 2011.